Vanishing vortex creep at the transition from ordered to disordered vortex phases in $Ba_{0.64}K_{0.36}Fe_2As_2$

Yu-Hao Liu,[1] Wei Xie,[1,2] and Hai-Hu Wen[1,*]

[1]*National Laboratory of Solid State Microstructures and Department of Physics, Collaborative Innovation Center of Advanced Microstructures, Nanjing University, Nanjing 210093, China*

[2]*Western Superconducting Technologies Company Ltd., Xi'an 710018, China*

(Received 22 January 2024; revised 17 March 2024; accepted 16 May 2024; published 3 June 2024)

By measuring the dynamical and conventional magnetization relaxation of $Ba_{0.64}K_{0.36}Fe_2As_2$ single crystals, we found a strong second peak effect on the magnetization hysteresis loops. It is found that there is a kink of magnetization at a field between the valley and maximum magnetization. Interestingly, the magnetization relaxation rate has a deep minimum at the field with the kink, indicating a diminished vortex creep. The relaxation rate at this field is clearly smaller than the so-called universal lower limit of the relaxation rate characterized by $S_0 \approx Gi^{1/2}(T/T_c)$. This diminished vortex creep is associated with the origin of the second magnetization peak effect and attributed to the strongly hindered flux motion when experiencing the transition from the quasi-ordered to disordered vortex phases.

DOI: 10.1103/PhysRevB.109.214503

I. INTRODUCTION

Since the discovery of superconductivity in $LaFeAsO_{1-x}F_x$ [1], iron-based superconductors have attracted considerable attention due to their unique properties and potential applications. Among iron-based superconductors, the optimally doped $Ba_{1-x}K_xFe_2As_2$ single crystal has a high superconducting transition temperature (T_c) [2,3], large critical current density (J_s) [4–6], a small anisotropy ratio (γ) [7–9], and samples are easy to fabricate [2,3]. A lot of studies on vortex dynamics were carried out on this type of sample [4–6,10–12]. One of the most interesting phenomena observed in $Ba_{1-x}K_xFe_2As_2$ single crystals is the second magnetization peak (SMP) effect, in which the width of magnetic hysteresis loops (MHLs) will increase with increasing magnetization and a second peak emerges far away from the zero field. This is of great significance for the high-field application of iron-based superconductors.

The SMP can be divided into three types according to the different shapes of MHLs. The first type occurs mainly in conventional superconductors, such as Nb [13], Nb_3Sn [14], $CeRu_2$ [15], 2H-$NbSe_2$ [15,16], and heavy fermion compounds [17]. The origin of this type is generally explained as the thermal melting of vortex lines and the enhancement of flux pinning [18,19], and the peak position is near the upper critical field H_{c2}.The second type occurs mainly in highly anisotropic cuprate superconductors, such as $Bi_2Sr_2CaCu_2O_{8+\delta}$ (Bi2212) [20] and $Bi_2Sr_2CuO_{6+\delta}$ (Bi2201) [21], and the peak in MHLs locates in a weak magnetic field and is temperature independent. The third type mainly occurs in $YBa_2Cu_3O_y$ (YBCO) [22], $Ba_{1-x}K_xBiO_3$ (BKBO) [23], and some iron-based superconductors [4–6,24], which is often referred to as the fishtail effect due to its shape, and the second peak position is strongly temperature dependent. Several theories have been proposed to explain the origin of the SMP effect, such as a crossover from elastic to plastic pinning as the field increases [25–27], structural phase transition of vortex lattices [28,29], and order-to-disorder vortex phase transition [22,30–32].

In $YBa_2Cu_3O_{7-\delta}$ (YBCO) crystals, a sharp kink has been observed between the valley (H_{dip}) and the second peak (H_p) of MHLs, and the field was named H_{kink} where the magnetic-field derivative dm/dH is the largest [33–35]. This phenomenon was interpreted as an order-disorder vortex phase transition and regarded to have a strong correlation with the origin of the SMP effect. Similarly, the Bragg peak has been observed in $Ba_{0.64}K_{0.36}Fe_2As_2$ single crystals by small-angle neutron scattering (SANS) measurement, which means a long-range ordered lattice exists at low field. As the magnetic field increases, the sharp Bragg peak crosses over to a diffraction ring, which was interpreted as an order-disorder transition concerning the SMP effect in MHLs [30]. Meanwhile, the vortex structure with short-range hexagonal order was observed in optimally doped $Ba_{0.6}K_{0.4}Fe_2As_2$, such as scanning tunneling microscopy (STM) [36] at high field ($H = 9$ T) and magnetic force microscopy (MFM) [37] at low field ($H < 100$ Oe).

In this study, we carry out systematic investigations on the magnetization relaxation rate of high-quality $Ba_{0.64}K_{0.36}Fe_2As_2$ single crystals. In the MHLs, a pronounced SMP effect and the kink can be observed. In studies on magnetization relaxation, a minimum value of magnetization relaxation rate can be observed at H_{kink}. The relaxation rate at the kink field is extremely small, indicating a very weak vortex motion. This observation provides evidence suggesting a potential association between the order-disorder transition and the SMP effect of iron-based superconductors.

*hhwen@nju.edu.cn

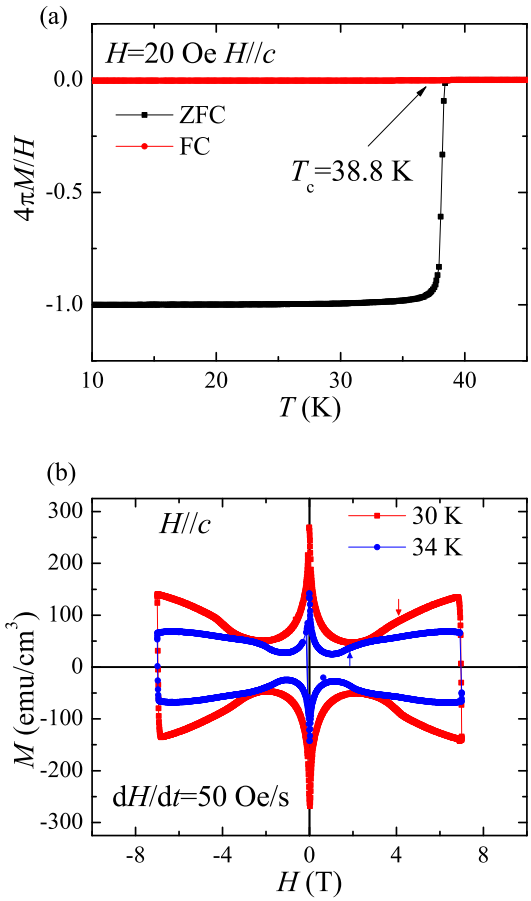

FIG. 1. Temperature dependence of magnetization and typical MHLs of $Ba_{0.64}K_{0.36}Fe_2As_2$ single crystal. (a) The superconducting transition curve obtained with zero-field-cooled and field-cooled modes at $H = 20$ Oe with $H//c$. (b) The isothermal MHLs of the sample with $dH/dt = 50$ Oe/s at 30 K (red) or 34 K (blue). The arrows indicate the kink positions on MHLs.

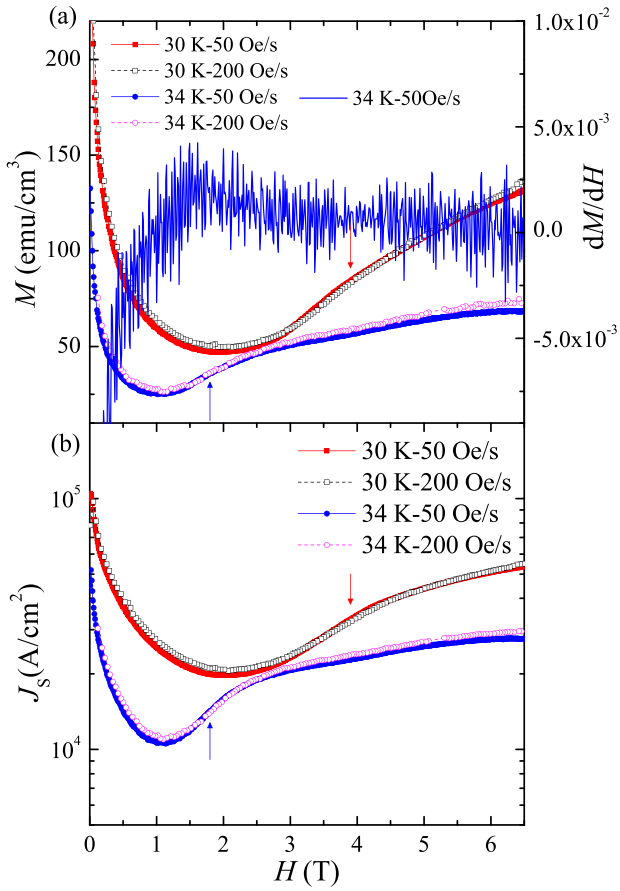

FIG. 2. Correlations of (a) MHLs and (b) J_s vs H for $Ba_{0.64}K_{0.36}Fe_2As_2$ single crystal at different temperatures with $dH/dt = 200$ Oe/s (open) and 50 Oe/s (solid). Arrows indicate the closest or intersecting position of the curves with different field-sweeping rates. The blue line in (a) is the magnetic-field derivative (dM/dH) at 34 K.

II. EXPERIMENTAL DETAILS

The $Ba_{0.64}K_{0.36}Fe_2As_2$ single crystals were grown by the self-flux method [2], with dimensions $1.6 \times 1.4 \times 0.14$ mm. The composition of the sample was characterized using scanning electron microscopy (SEM) conducted on Phenom ProX (Phenom). The dc magnetization measurements were carried out with a SQUID-VSM-7T (Quantum Design). The magnetic field H was applied parallel to the c axis of the single crystal. In the dynamical magnetization relaxation measurements [38], the MHLs were measured in magnetic fields up to 7 T with different sweeping rates ($dH/dt = 200$ Oe/50 Oe). In the conventional magnetization relaxation measurements [39], the sample was zero-field cooled down from above T_c to the desired temperature, and then the magnetic field was quickly increased to a certain value. The magnetization measurements started immediately after the certain fields were applied, and the measuring time was 3 h.

III. RESULTS AND DISCUSSION

Figure 1(a) shows the temperature dependence of magnetization of the $Ba_{0.64}K_{0.36}Fe_2As_2$ single crystal with the zero-field-cooled (ZFC) and field-cooled (FC) modes. The magnetic field is 20 Oe and parallel to the c axis of the sample. The sharp transition indicates that the sample is of high quality, and after taking the demagnetization factor into account, the magnetic shielding volume should be 100%. The obtained superconducting transition temperature is 38.8 K, which is determined as the intersection of the magnetization in ZFC and FC modes in Fig. 1(a).The MHLs for the $Ba_{0.64}K_{0.36}Fe_2As_2$ single crystal were measured at different temperatures. The results measured at 30 K or 34 K with $dH/dt = 50$ Oe/s are shown in Fig. 1(b). The MHLs exhibit a symmetric shape as a result of strong bulk pinning. The values of H_{kink} at 30 K and 34 K are 3.9 T and 1.8 T, respectively. The H_{kink} of the $Ba_{0.64}K_{0.36}Fe_2As_2$ in Fig. 1(b) decreases gradually with increasing temperature, which is different from YBCO [35], and this may be caused by different pinning mechanisms of the two superconductors.

Shown in Fig. 2(a) are the MHLs measured in the field ascending processes with different field-sweeping rates. At each temperature, an anomalous intersection between $M(H)$ curves with different field-sweeping rates is observed. Taking the scenario at 34 K as an example, this characteristic

magnetic field nearly coincides with the peak of the magnetic-field derivative (dM/dH) as shown in Fig. 2(a). To eliminate the influence of equilibrium magnetization, we calculated the superconducting current density by the Bean critical state model J_s=20$\Delta M/w$(1-w/3l), where ΔM= M_+-M_-, M_+(M_-) is the magnetization associated with descending (ascending) field, l is the length, and w is the width of the single crystal ($l > w$) [40]. The results are shown in Fig. 2(b). As one can see, double crossings of the isothermal MHL curves occur in the near region of the kink at $H_{\rm kink}$. It shows that the magnetization width ΔM is even getting narrower measured with a high sweeping rate than that with a lower sweeping rate. This is abnormal, indicating a "negative" relaxation rate in the field-sweeping process. In the field-sweeping process, it is known that, if dM/dt is much smaller than $E \propto dB/dt$, then combining with the thermally activated flux creep model,

$$E = v_0 B \exp\left[-\frac{U(T,j)}{k_B T}\right], \tag{1}$$

and the Kim-Anderson model, $U(T, j)$=$U_c(T)$[1 − $j/j_c(T)$], one can get the relation

$$j = j_c(T)\left[1 - \frac{k_B T}{U_c(T)} \ln\left(\frac{v_0 B}{E}\right)\right], \tag{2}$$

where $U(T, B)$ is the activation energy and v_0 is the attempting hopping velocity. One can see that a larger field-sweeping rate should correspond to a larger E and a larger transient current density j. And, according to the Bean critical state model, the width of the MHL should be larger. This clearly indicates that the MHLs measured with a higher field-sweeping rate should always be wider than those with a lower sweeping rate. Thus, the crossings of the MHLs measured with different sweeping rates shown in Fig. 2 are abnormal. For a thin disk, $dM/dt << dB/dt$, a good approximation can be established [41,42],

$$U(T,B) = k_B T ln\left(\frac{2v_0 B}{w(dB/dt)}\right). \tag{3}$$

Here, w is the width of the sample. Equation (3) indicates that a faster sweeping rate corresponds to a smaller activation energy, thus expecting a larger j value and a wider MHL, again showing that the intersection of MHLs with different field-sweeping rates is unreasonable. Taking into account the nonuniform distribution of the magnetic field in the sample, we believe this may be a fake observation, namely, a smaller width of MHL corresponds to a larger sweeping rate. But, at least it shows a negligible relaxation effect near the kink field. To comprehend the physics concerning the flux dynamics near the kink, we calculate the dynamical magnetization relaxation rate Q, which is defined as

$$Q = \frac{dln(J_s)}{dln(dB/dt)} = \frac{dln(\Delta M)}{dln(dB/dt)}. \tag{4}$$

The parameter Q is calculated by Eq. (4), in which J_s is measured with two different field-sweeping rates, 50 and 200 Oe/s. The results of 30 K, 32 K, and 34 K are shown in Fig. 4(a). One can see negative values of Q near the kink on the MHL.

To better understand the physics concerning the vortex motion near the kink, we measured the magnetization relaxation

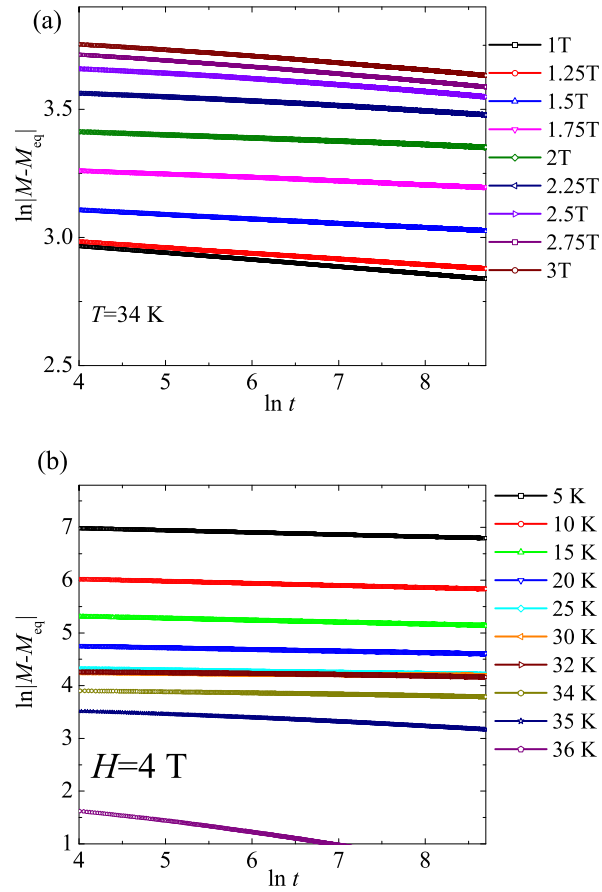

FIG. 3. Double-logarithmic plots of the time dependence of magnetization at (a) various fields at $T = 34$ K and (b) different temperatures at $H = 4$T.

and determined the relaxation rate S, namely, the time dependence of magnetization is measured. The S is determined through

$$S = -\frac{dln(|M - M_{\rm eq}|)}{dlnt}, \tag{5}$$

where $M_{\rm eq} = (M_+ + M_-)/2$ is the equilibrium magnetization obtained from the MHLs at the same temperature. In order to investigate the field dependence of S, we measured the $M(t)$ at 30 K, 32 K, and 34 K with different applied fields. The calculated results are shown in Fig. 4(a) by the solid symbols. For each field and temperature, the measuring time was 10 800 s (3 h). The double-logarithmic plots of $M(t)$ at 34 K are shown in Fig. 3(a). When the field increases to 2T, the slope decreases to a small value. This suggests a clear smaller conventional relaxation rate at 2T when the temperature is T = 34 K, as shown in Fig. 4(a). Similarly, we measured the $M(t)$ with a certain field at different temperatures. Three fields are chosen: 2T, 3T, 4T, and the results of 4T are shown in Fig. 3(b). The slope of the curve decreases with increasing temperature below 30 K, but above 30 K the opposite trend is observed, indicating a smaller relaxation rate near the field of temperature where the kink of the MHL appears. Thus, both the dynamical relaxation and conventional relaxation of magnetization all indicate a strongly suppressed relaxation

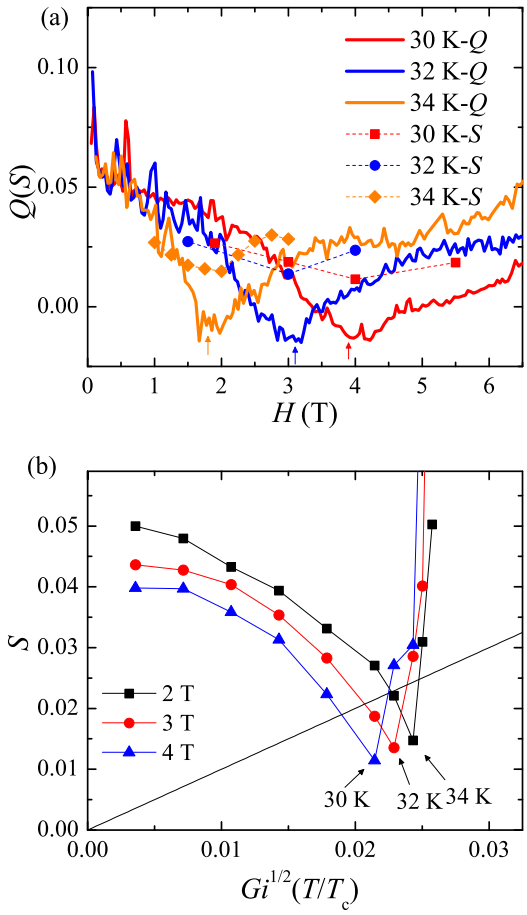

FIG. 4. (a) Field dependence of relaxation rate Q (solid line) and S (dashed line) at different magnetic temperatures. Arrows indicate the minimum values of the magnetization relaxation rates at different temperatures. (b) The plots of S vs $Gi^{1/2}(T/T_c)$, which indicate that a characteristic temperature where S is minimum exists at a fixed magnetic field.

rate near the kink, which we attribute to crossover of different vortex phases.

In the single-vortex regime, the activation energy U_{sv} is equal to the pinning energy E_{pin}, which can be expressed as $E_{pin} = (\gamma\xi^2 L_c)^{1/2}$. Here, γ is the disorder parameter, ξ is the coherence length, and L_c is the collective pinning length. We can express $U_{sv} = H_c^2\xi^4/L_c$ via the elastic energy $U_{sv} = U_e = \epsilon_0\xi^2/L_c$ and $H_c = \Phi_0/2\sqrt{2}\pi\lambda\xi$, where H_c is the thermodynamic critical field, ϵ_0 is an important energy scale which determines the self-energy of the vortex lines and can be given by $\epsilon_0 = (\Phi_0/4\pi\lambda)^2$, λ is the penetration depth, and $\Phi_0 = h/2e$ is the flux quantum. By introducing the Ginzburg number in the form of $Gi = (T_c/H_c^2\epsilon\xi^3)^2/2$ and a very common relation $(\epsilon\epsilon_0\xi/T_c)^2 = (1 - T/T_c)/8Gi$, with ϵ as the anisotropy parameter, the activation energy U_{sv} can be rewritten as $U_{sv} = T_c\xi[(1-t)/Gi]^{1/2}/L_c$, where t is the reduced temperature T/T_c [43]. When the current j reaches the critical current density j_c, the pinning force $(\gamma L_c)^{1/2}$ is equal to the Lorentz force $j_c\Phi_0 L_c$; then, we can obtain the $\xi/L_c = (j_c/j_0)^{1/2}$, where j_0 is the depairing current density. Finally, the U_{sv} can be written as $T_c[(1-t)/Gi]^{1/2}(j_c/j_0)^{1/2}$ [19]. The effective pinning energy is typically defined in the form of $U = T/S$, so the $S = t[Gi/(1-t)]^{1/2}(j_0/j_c)^{1/2}$ is considered to be larger than $Gi^{1/2}(T/T_c)$ due to $j_0 > j_c$ and $t < 1$ [19,44]. A noteworthy observation on curve $S(T, B)$ is that there is a clear minimum. Taking the related parameters of the present superconductor, we found that $S(T, B)$ increases linearly with temperature T. The comparison of $S(T)$ and $Gi^{1/2}(T/T_c)$ is shown in Fig. 4(b). It is evident that the minimum relaxation rate is even lower than the lower limit of $Gi^{1/2}(T/T_c)$. We attribute this very low relaxation rate to the heavily damped vortex motion near the kink region, thus it is most likely related to a vortex phase transition. Considering the ordered vortex pattern observed in the low field region, we anticipate that the vortex structure undergoes a transition from a quasi-ordered (such as Bragg glass state) to a more disordered state. It is the enhanced entanglement of vortices near the kink that produces the very small relaxation rate, as shown in Fig. 4(a). It is found that once the second peak effect appears on the MHL curve, the local minimum of the relaxation rate emerges. This implies that once the magnetic field surpasses H_{dip}, the vortex creep cannot be described by the single vortex pinning of the collective pinning model anymore, and strong entanglement of vortices starts to occur. When the field is higher than H_{kink}, the relaxation rate increases again for the system going to another phase, most likely in the vortex glass state.

Although Q and S are obtained through two different methods, we can see that they are almost equal to each other, providing similar information of vortex dynamics [42,45]. Figure 4(a) shows the field dependence of Q and S. They both exhibit a minimum value at the same field, indicated by the arrows. The position of the minimum coincides with the H_{kink} at all temperatures. Hence, it reveals that the kinks observed in MHLs and the minima observed in the relaxation rate curves are attributable to the same vortex structure transformations. In $YBa_2Cu_3O_{7-\delta}$ (YBCO) crystals, kinks were also observed on the MHL curves and interpreted as an order-disorder vortex phases transition [34]. At low temperatures and fields, the vortex structures often exhibit a quasi-ordered state, such as the Bragg glass. However, as the temperature increases or the magnetic field intensifies, a more disordered vortex phase is observed. There are different physical considerations, and thus expressions for the specific location of the phase transition, such as the magnetic field at which the vortex elastic energy E_{el} equals the pinning energy E_{pin} [34,35] or the Bragg peak completely disappears [30]. These descriptions, in essence, are consistent with each other. As the temperature or the field increases, the flux lines become entangled and disordered. Simultaneously, the relaxation rate of vortex creep decreases, leading to an increase in the critical current density. When the field approaches H_p, the system is still in the vortex glass state, and the relaxation rate increases or remains flat, but the critical current density becomes higher due to the enhanced entanglement of vortices. However, when the field is beyond the peak field of magnetization, the flux lines start to break, yielding some dislocations of the vortex, and the system enters the plastic motion regime. In this regime, the relaxation rate increases rapidly, and the critical current density drops down quickly. Figure 5 shows the phase diagram of the

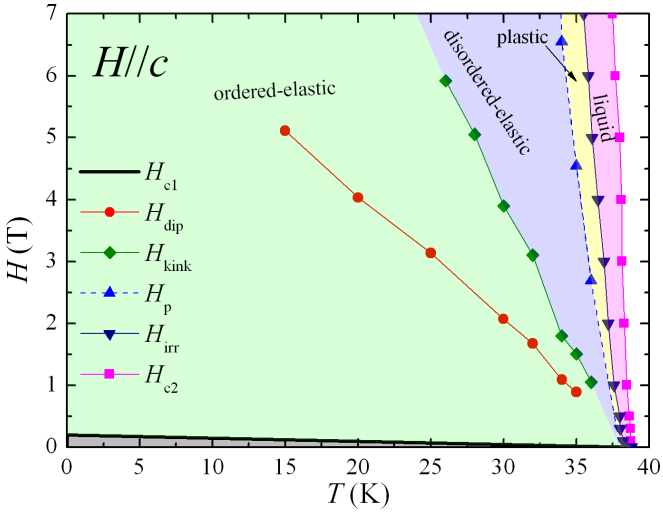

FIG. 5. Phase diagram of $Ba_{0.64}K_{0.36}Fe_2As_2$ single crystals. The black line is a sketch of the lower critical field H_{c1}. The red circles are the H_{dip} obtained by the minimum value of $J_s(H)$ at different temperatures. The green diamonds are the field H_{kink}, which is the boundary of the ordered-elastic region and disordered-elastic region. The blue up-triangles are the field H_p, which is the boundary of the elastic region and plastic region. The dashed line is a guide to the eye. The navy down-triangles are the irreversibility field H_{irr}. The magenta squares are the upper critical field H_{c2}.

$Ba_{0.64}K_{0.36}Fe_2As_2$ single crystal when the magnetic field H was applied parallel to the c axis. The black line is the sketch of the lower critical field $H_{c1}(T)$, and the gray region below $H_{c1}(T)$ is the Meissner state. In the green region between $H_{kink}(T)$ and $H_{c1}(T)$, when the magnetic flux lines initially penetrate into the bulk area of the sample, their motion is rapid, leading to the emergence of a peak at low field on the $Q(H)$ curves [10]. As the density of flux lines gradually increases, the vortex structure undergoes a phase transition from an ordered to a disordered phase, and a vortex glass state with vortex entanglement appears above H_{kink}. In the blue region between $H_{kink}(T)$ and $H_p(T)$, it is in the vortex glass state with strong entanglement of vortices. Above H_p, the entangled flux lines gradually break and cut each other, and the vortex system goes into a plastic flow regime. The irreversibility field $H_{irr}(T)$ is defined as the points where the ZFC and FC magnetization intersect with each other, showing a boundary for the free flux flow. The upper critical field $H_{c2}(T)$ is defined as the starting point of the formation of the superconducting droplet, corresponding to the field where the magnetization deviates from the paramagnetic normal state background in $M(T)$ curves. We define the yellow region between $H_p(T)$ and $H_{irr}(T)$ as the plastic motion region and the magenta region between $H_{irr}(T)$ and $H_{c2}(T)$ as the vortex liquid, respectively. Both regions are small. When the field exceeds $H_{c2}(T)$, the sample is in the normal state.

IV. CONCLUSIONS

In summary, we have measured the dynamical and conventional magnetization relaxation rates of the $Ba_{0.64}K_{0.36}Fe_2As_2$ single crystal. The magnetic field dependence of both relaxation rates exhibits a minimum value at the same field. This point corresponds to a diminished vortex creep with a relaxation rate smaller than the so-called universal lower limit of the relaxation rate. This is attributed to the transition from ordered (Bragg glass) to disordered vortex (such as vortex glass) phases. Above the peak position, the dislocations of the vortex proliferate quickly, leading to a rapid increase in the relaxation rate and a decrease in the critical current density. Further work is warranted, with a particular interest in the local magnetization measurements, which could more directly measure the order-disorder transition lines.

ACKNOWLEDGMENTS

This work is supported by the National Natural Science Foundation of China (Grants No. A0402/11927809 and No. A0402/11534005), National Key R and D Program of China (Grant No. 2022YFA1403201), and the Strategic Priority Research Program (B) of Chinese Academy of Sciences (Grant No. XDB25000000).

[1] Y. Kamihara, T. Watanabe, M. Hirano, and H. Hosono, Iron-based layered superconductor $La[O_{1-x}F_x]FeAs$ ($x = 0.05 - 0.12$) with $T_c = 26$ K, J. Am. Chem. Soc. **130**, 3296 (2008).

[2] H. Luo, Z. Wang, H. Yang, P. Cheng, X. Zhu, and H. H. Wen, Growth and characterization of $A_{1-x}K_xFe_2As_2$ (A = Ba, Sr) single crystals with $x = 0-0.4$, Supercond. Sci. Technol. **21**, 125014 (2008).

[3] A. S. Sefat, R. Jin, M. A. McGuire, B. C. Sales, D. J. Singh, and D. Mandrus, Superconductivity at 22 K in Co-doped $BaFe_2As_2$ crystals, Phys. Rev. Lett. **101**, 117004 (2008).

[4] S. Ishida, D. Song, H. Ogino, A. Iyo, H. Eisaki, M. Nakajima, J. Shimoyama, and M. Eisterer, Doping-dependent critical current properties in K, Co, and P-doped $BaFe_2As_2$ single crystals, Phys. Rev. B **95**, 014517 (2017).

[5] H. Yang, H. Luo, Z. Wang, and H. H. Wen, Fishtail effect and the vortex phase diagram of single crystal $Ba_{0.6}K_{0.4}Fe_2As_2$, Appl. Phys. Lett. **93**, 142506 (2008).

[6] Y. Liu, 1, L. Zhou, K. Sun, W. E. Straszheim, M. A. Tanatar, R. Prozorov, and T. A. Lograsso, Doping evolution of the second magnetization peak and magnetic relaxation in $(Ba_{1-x}K_x)Fe_2As_2$ single crystals, Phys. Rev. B **97**, 054511 (2018).

[7] M. Putti, I. Pallecchi, E. Bellingeri, M. R. Cimberle, M. Tropeano, C. Ferdeghini, A. Palenzona, C. Tarantini, A. Yamamoto, J. Jiang, J. Jaroszynski, F. Kametani, D. Abraimov, A. Polyanskii, J. D. Weiss, E. E. Hellstrom, A. Gurevich, D. C. Larbalestier, R. Jin *et al.*, New Fe-based superconductors: Properties relevant for applications, Supercond. Sci. Technol. **23**, 034003 (2010).

[8] M. M. Altarawneh, K. Collar, C. H. Mielke, N. Ni, S. L. Bud'ko, and P. C. Canfield, Determination of anisotropic H_{c2} up to 60 T in $Ba_{0.55}K_{0.45}Fe_2As_2$ single crystals, Phys. Rev. B **78**, 220505(R) (2008).

[9] M. Kano, Y. Kohama, D. Graf, F. Balakirev, A. S. Sefat, M. A. McGuire, B. C. Sales, D. Mandrus, and S. W. Tozer, Anisotropy of the upper critical field in a Co-doped $BaFe_2As_2$ single crystal, J. Phys. Soc. Jpn. **78**, 084719 (2009).

[10] W. Cheng, H. Lin, B. Shen, and H. H. Wen, Comparative study of vortex dynamics in $CaKFe_4As_4$ and $Ba_{0.6}K_{0.4}Fe_2As_2$ single crystals, Sci. Bull. **64**, 81 (2019).

[11] B. Shen, P. Cheng, Z. Wang, L. Fang, C. Ren, L. Shan, and H. H. Wen, Flux dynamics and vortex phase diagram in $Ba(Fe_{1-x}Co_x)_2As_2$ single crystals revealed by magnetization and its relaxation, Phys. Rev. B **81**, 014503 (2010).

[12] A. K. Pramanik, L. Harnagea, S. Singh, S. Aswartham, G. Behr, S. Wurmehl, C. Hess, R. Klingeler, and B. Büchner, Critical current and vortex dynamics in single crystals of $Ca(Fe_{1-x}Co_x)_2As_2$, Phys. Rev. B **82**, 014503 (2010).

[13] X. S. Ling, S. R. Park, B. A. McClain, S. M. Choi, D. C. Dender, and J. W. Lynn, Superheating and supercooling of vortex matter in a Nb single crystal: Direct evidence for a phase transition at the peak effect from neutron diffraction, Phys. Rev. Lett. **86**, 712 (2001).

[14] R. Lortz, N. Musolino, Y. Wang, A. Junod, and N. Toyota, Origin of the magnetization peak effect in the Nb_3Sn superconductor, Phys. Rev. B **75**, 094503 (2007).

[15] S. S. Banerjee, N. G. Patil, S. Saha, S. Ramakrishnan, A. K. Grover, S. Bhattacharya, G. Ravikumar, P. K. Mishra, T. V. C. Rao, V. C. Sahni, M. J. Higgins, E. Yamamoto, Y. Haga, M. Hedo, Y. Inada, and Y. Onuki, Anomalous peak effect in $CeRu_2$ and 2H-$NbSe_2$: Fracturing of a flux line lattice, Phys. Rev. B **58**, 995 (1998).

[16] S. Bhattacharya and M. J. Higgins, Dynamics of a disordered flux line lattice, Phys. Rev. Lett. **70**, 2617 (1993).

[17] K. Tenya, M. Ikeda, T. Tayama, T. Sakakibara, E. Yamamoto, K. Maezawa, N. Kimura, R. Settai, and Y. Onuki, Anisotropic magnetic response in the superconducting mixed state of UPt_3, Phys. Rev. Lett. **77**, 3193 (1996).

[18] A. B. Pippard, A possible mechanism for the peak effect in type II superconductors, Philos. Mag. **19**, 217 (1969).

[19] G. Blatter, M. V. Feigelman, V. B. Geshkenbein, A. I. Larkin, and V. M. Vinokur, Vortices in high-temperature superconductors, Rev. Mod. Phys. **66**, 1125 (1994).

[20] B. Khaykovich, E. Zeldov, D. Majer, T. W. Li, P. H. Kes, and M. Konczykowski, Vortex-lattice phase transitions in $Bi_2Sr_2CaCu_2O_8$ crystals with different oxygen stoichiometry, Phys. Rev. Lett. **76**, 2555 (1996).

[21] A. Piriou, E. Giannini, Y. Fasano, C. Senatore, and Ø. Fischer, Vortex phase diagram and temperature-dependent second-peak effect in overdoped $Bi_2Sr_2CuO_{6+\delta}$ crystals, Phys. Rev. B **81**, 144517 (2010).

[22] K. Deligiannis, P. A. J. de Groot, M. Oussena, S. Pinfold, R. Langan, R. Gangon, and L. Taillefer, New features in the vortex phase diagram of $YBa_2Cu_3O_{7-\delta}$, Phys. Rev. Lett. **79**, 2121 (1997).

[23] Y. Jiao, W. Cheng, Q. Deng, H. Yang, H. H. Wen, Collective vortex pinning and merging of the irreversibility line and second peak effect in optimally doped $Ba_{1-x}K_xBiO_3$ single crystals, Physica C **545**, 43 (2018).

[24] M. Bonura, E. Giannini, R. Viennois, and C. Senatore, Temperature and time scaling of the peak-effect vortex configuration in $FeTe_{0.7}Se_{0.3}$, Phys. Rev. B **85**, 134532 (2012).

[25] Y. Abulafia, A. Shaulov, Y. Wolfus, R. Prozorov, L. Burlachkov, Y. Yeshurun, D. Majer, E. Zeldov, H. Wühl, V. B. Geshkenbein, and V. M. Vinokur, Plastic vortex creep in $YBa_2Cu_3O_{7-x}$ crystals, Phys. Rev. Lett. **77**, 1596 (1996).

[26] R. Prozorov, N. Ni, M. A. Tanatar, V. G. Kogan, R. T. Gordon, C. Martin, E. C. Blomberg, P. Prommapan, J. Q. Yan, S. L. Bud'ko, and P. C. Canfield, Vortex phase diagram of $Ba(Fe_{0.93}Co_{0.07})_2As_2$ single crystals, Phys. Rev. B **78**, 224506 (2008).

[27] S. Salem-Sugui, L. Ghivelder, A. D. Alvarenga, L. F. Cohen, K. A. Yates, K. Morrison, J. L. Pimentel, H. Luo, Z. Wang, and H. H. Wen, Flux dynamics associated with the second magnetization peak in the iron pnictide $Ba_{1-x}K_xFe_2As_2$, Phys. Rev. B **82**, 054513 (2010).

[28] B. Rosenstein, B. Ya. Shapiro, I. Shapiro, Y. Bruckental, A. Shaulov, and Y. Yeshurun, Peak effect and square-to-rhombic vortex lattice transition in $La_{2-x}Sr_xCuO_4$, Phys. Rev. B **72**, 144512 (2005).

[29] R. Kopeliansky, A. Shaulov, B. Ya. Shapiro, and Y. Yeshurun, B. Rosenstein, J. J. Tu, L. J. Li, G. H. Cao, and Z. A. Xu, Possibility of vortex lattice structural phase transition in the superconducting pnictide $Ba(Fe_{0.925}Co_{0.075})_2As_2$, Phys. Rev. B **81**, 092504 (2010).

[30] S. Demirdiş, C. J. van der Beek, S. Mühlbauer, Y. Su, and Th. Wolf, SANS study of vortex lattice structural transition in optimally doped $(Ba_{1-x}K_x)Fe_2As_2$, J. Phys.: Condens. Matter **28**, 425701 (2016).

[31] A. van Otterlo, R. T. Scalettar, and G. T. Zimányi, Dynamic phases and the peak effect in dirty type II superconductors, Phys. Rev. Lett. **84**, 2493 (2000).

[32] D. Giller, A. Shaulov, R. Prozorov, Y. Abulafia, Y. Wolfus, L. Burlachkov, Y. Yeshurun, E. Zeldov, V. M. Vinokur, J. L. Peng, and R. L. Greene, Disorder-induced transition to entangled vortex solid in Nd-Ce-Cu-O crystal, Phys. Rev. Lett. **79**, 2542 (1997).

[33] Y. Radzyner, S. B. Roy, D. Giller, Y. Wolfus, A. Shaulov, P. Chaddah, and Y. Yeshurun, Metastable vortex states in $YBa_2Cu_3O_{7-\delta}$ crystal, Phys. Rev. B **61**, 14362 (2000).

[34] D. Giller, A. Shaulov, Y. Yeshurun, and J. Giapintzakis, Vortex solid-solid phase transition in an untwinned $YBa_2Cu_3O_{7-\delta}$ crystal, Phys. Rev. B **60**, 106 (1999).

[35] T. Nishizaki, T. Naito, S. Okayasu, A. Iwase, and N. Kobayashi, Effects of weak point disorder on the vortex matter phase diagram in untwinned $YBa_2Cu_3O_y$ single crystals, Phys. Rev. B **61**, 3649 (2000).

[36] L. Shan, Y. Wang, B. Shen, B. Zeng, Y. Huang, A. Li, D. Wang, H. Yang, C. Ren, Q. Wang, S. H. Pan, and H. H. Wen, Observation of ordered vortices with Andreev bound states in $Ba_{0.6}K_{0.4}Fe_2As_2$, Nat. Phys. **7**, 325 (2011).

[37] H. Yang, B. Shen, Z. Wang, L. Shan, C. Ren, and H. H. Wen, Vortex images on $Ba_{1-x}K_xFe_2As_2$ observed directly by magnetic force microscopy, Phys. Rev. B **85**, 014524 (2012).

[38] M. Jirsa, L. Pust, H. G. Schnack, and R. Griessen, Extension of the time window for investigation of relaxation effects in high-T_c superconductors, Physica C **207**, 85 (1993).

[39] Y. Yeshurun, A. P. Malozemoff, and A. Shaulov, Magnetic relaxation in high-temperature superconductors, Rev. Mod. Phys. **68**, 911 (1996).

[40] C. P. Bean, Magnetization of high-field superconductors, Rev. Mod. Phys. **36**, 31 (1964).

[41] H. G. Schnack, J. G. Lensink, R. Griessen, C. J. van der Beek, and P. H. Kes, Magnetization and relaxation curves of fast relaxing high-T_c superconductors, Phys. C **197**, 337 (1992).

[42] H. H. Wen, H. G. Schnack, R. Griessen, B. Dam, and J. Rector, Critical current, magnetization relaxation and activation energies for $YBa_2Cu_3O_7$ and $YBa_2Cu_4O_8$ films, Physica C **241**, 353 (1995).

[43] A. Larkin and A. Varlamov, *Theory of Fluctuations in Superconductors* (Oxford University Press, Oxford, 2005).

[44] S. Eley, M. Miura, B. Maiorov, and L. Civale, Universal lower limit on vortex creep in superconductors, Nat. Mater. **16**, 409 (2017).

[45] A. J. J. van Dalen, M. R. Koblischka, and R. Griessen, Equivalence of dynamical and conventional magnetic relaxation in high-T_c superconductors, Physica C **259**, 157 (1996).